Published in final edited form as:

Nature. ; 477(7362): 90–94. doi:10.1038/nature10357.

The aging systemic milieu negatively regulates neurogenesis and cognitive function

Saul A. Villeda[1,2], **Jian Luo**[1], **Kira I. Mosher**[1,2], **Bende Zou**[3], **Markus Britschgi**[1,#], **Gregor Bieri**[1,4], **Trisha M. Stan**[1,5], **Nina Fainberg**[1], **Zhaoqing Ding**[1,5], **Alexander Eggel**[1], **Kurt M. Lucin**[1], **Eva Czirr**[1], **Jeong-Soo Park**[1], **Sebastien Couillard-Després**[6], **Ludwig Aigner**[6], **Ge Li**[7], **Elaine R. Peskind**[7,8], **Jeffrey A. Kaye**[9], **Joseph F. Quinn**[9], **Douglas R. Galasko**[10], **Xinmin S. Xie**[3], **Thomas A. Rando**[1,11,12], and **Tony Wyss-Coray**[1,2,5,11,*]

[1]Department of Neurology and Neurological Sciences, Stanford University School of Medicine, Stanford, California 94305, USA [2]Neuroscience IDP Program, Stanford University School of Medicine, Stanford, California 94305, USA [3]AfaSci Research Laboratory, Redwood City, California, 94063, USA [4]School of Life Sciences, Swiss Federal Institute of Technology (EPFL), CH-1015 Lausanne, Switzerland [5]Immunology IDP Program, Stanford University School of Medicine, Stanford, California 94305, USA [6]Institute of Molecular Regenerative Medicine, Paracelsus Medical University, Strubergasse 21, A-5020 Salzburg, Austria [7]Dept. of Psychiatry and Behavioral Sciences, University of Washington School of Medicine, Seattle, WA 98108-1597, USA [8]Veterans Affairs Northwest Network Mental Illness Research, Education, and Clinical Center, Seattle, WA 98108-1597, USA [9]Layton Aging & Alzheimer's Disease Center, Oregon Health and Science University, CR131, 3181 SW Sam Jackson Park Road, Portland, OR 97201-3098, USA and Portland VA Medical Center, Portland, OR 97207 [10]Department of Neurosciences, University of California San Diego, 9500 Gilman Drive #0948, La Jolla, CA 92093-0948, USA [11]Center for Tissue Regeneration, Repair and Restoration, VA Palo Alto Health Care System, Palo Alto, California 94304, USA [12]The Glenn Laboratories for the Biology of Aging, Stanford University School of Medicine, Stanford, CA 94305, USA

Summary

In the central nervous system (CNS), aging results in a precipitous decline in adult neural stem/progenitor cells (NPCs) and neurogenesis, with concomitant impairments in cognitive functions[1]. Interestingly, such impairments can be ameliorated through systemic perturbations such as

*Corresponding Author: twc@stanford.edu.

#Current address: CNS Discovery, pRED, F. Hoffmann-La Roche Ltd., Basel, Switzerland

Author Contributions. S.A.V and T.W.C developed the concept and designed all experiments. S.A.V and J.L designed and performed in vivo experiments. S.A.V performed behavioral experiments. K.I assisted with surgery. B.Z and X.X performed electrophysiology. M.B and A.E. analyzed human data. G.B assisted with fear conditioning and irradiation analysis. S.A.V, T.M.S and J.S.P performed in vitro experiments. T.M.S assisted with MCSF analysis. N.F. assisted with radial arm maze. Z.D performed flow cytometry. K.M.L performed irradiation. E.C assisted with in vivo plasma experiments. D.R.G, G.L, E.R.P, J.A.K and J.F.Q identified aging subjects and provided human samples. S.C-D and L.A provided reagents and mice. T.A.R provided reagents, conceptual advice and edited manuscript. S.A.V collected data, performed data analysis, and generated figures. S.A.V and T.W.C wrote manuscript. T.W.C supervised all aspects of this project. All authors had the opportunity to discuss results and comment on manuscript.

Competing Interests Statement: The authors declare that they have no competing financial interests.

exercise[1]. Here, using heterochronic parabiosis we show that blood-borne factors present in the systemic milieu can inhibit or promote adult neurogenesis in an age dependent fashion in mice. Accordingly, exposing a young animal to an old systemic environment, or to plasma from old mice, decreased synaptic plasticity and impaired contextual fear conditioning and spatial learning and memory. We identify chemokines - including CCL11/Eotaxin – whose plasma levels correlate with reduced neurogenesis in heterochronic parabionts and aged mice, and whose levels are increased in plasma and cerebral spinal fluid of healthy aging humans. Finally, increasing peripheral CCL11 chemokine levels in vivo in young mice decreased adult neurogenesis and impaired learning and memory. Together our data indicate that the decline in neurogenesis, and cognitive impairments, observed during aging can be in part attributed to changes in blood-borne factors.

Adult neurogenesis occurs in local microenvironments, or neurogenic niches in the subventricular zone (SVZ) of the lateral ventricles and the subgranular zone (SGZ) of the hippocampus[2,3]. Permissive cues within the neurogenic niche are thought to drive the production of new neurons and their subsequent integration into the neurocircuitry of the brain[4,5], directly contributing to cognitive processes including learning and memory[6–8,9]. Importantly, the neurogenic niche is localized around blood vessels[10,11], allowing for potential communication with the systemic environment. Therefore, the possibility arises that diminished neurogenesis during aging may be modulated by the balance of two independent forces – intrinsic CNS-derived cues[12–14], and cues extrinsic to the CNS delivered by blood. Thus we hypothesized that age-related systemic molecular changes could cause a decline in neurogenesis and impair cognitive function during aging.

We first characterized cellular, electrophysiological and behavioral changes associated with the neurogenic niche in the dentate gyrus (DG) of the hippocampus in an aging cohort of mice. We observed cellular changes consistent with dramatically decreased adult neurogenesis[1] and increased neuroinflammation with age[15] (Supplementary Fig. 2a–e). Additionally, we detected deficits in synaptic plasticity (Supplementary Fig. 3a–c), and behavioral deficits in contextual fear conditioning (Supplementary Fig. 4a–c) and radial arm water maze (RAWM; Supplementary Fig. 4d–f) paradigms in old animals, consistent with decreased cognitive function during aging[16].

Next we investigated the contribution of peripheral systemic factors to the age-related decline in neurogenesis in the DG of the hippocampus in the setting of isochronic (young-young and old-old) and heterochronic (young-old) parabiosis (Fig. 1a). Remarkably, the number of Doublecortin (Dcx)-positive newly born neurons (Fig. 1b,c), BrdU-positive cells (Fig. 1e,f), and Sox2-positive progenitors (Supplementary Fig. 5a,b) decreased in young heterochronic parabionts. In contrast, we observed an increase in the number of Dcx-positive (Fig. 1b,d), BrdU-positive (Fig. 1e,g) and Sox2-positive (Supplementary Fig. 5a,c) cells in the old heterochronic parabionts. The number of Dcx-positive neurons between unpaired age-matched animals and isochronic animals showed no difference (Supplementary Fig. 6a,b). As a control flow cytometry analysis confirmed a shared vasculature in a subset of parabiotic pairs, in which one parabiont was transgenic for green fluorescent protein (GFP, Supplementary Fig. 7a–d). Together our findings suggest that global age-dependent

systemic changes can modulate neurogenesis in both the young and aged neurogenic niche, potentially contributing to the decline in regenerative capacity observed in the normal aging brain.

As previously reported by others[17], we rarely detected peripherally derived GFP cells in the CNS of wild-type mice, and these numbers did not differ between isochronic and heterochronic pairings (Supplementary Fig. 7e), suggesting the observed effects are mediated by soluble factors in plasma. To confirm that circulating factors within aged blood contribute to reduced neurogenesis with age, we intravenously injected plasma isolated from young or old mice into young adult animals (Fig 2a). The number of Dcx-positive cells in the DG decreased in animals receiving old plasma compared to animals receiving young plasma (Fig 2b,c), indicating that soluble factors present in old blood inhibit adult neurogenesis.

To investigate the functional effect of the aging systemic milieu, extracellular electrophysiological recordings were done on hippocampal slices prepared from young isochronic and heterochronic parabionts (Fig. 1h,i, Supplementary Fig. 6c). A decrease in long-term potentiation (LTP) in the DG of heterochronic parabionts was detected (Fig. 1h,i). These data indicate that age-related systemic changes can elicit deficits in synaptic plasticity. As LTP is considered a correlate of learning and memory[18], these finding suggest that age-related systemic changes may also impact cognitive functions during aging.

Subsequently, we tested hippocampal dependent learning and memory using contextual fear conditioning and RAWM paradigms in young adult mice intravenously injected with young or old plasma (Fig 2d,e). During fear conditioning training mice exhibited no differences in baseline freezing regardless of plasma injection treatment (Supplementary Fig. 8a). However, mice receiving old plasma demonstrated decreased freezing in contextual (Fig. 2d), but not cued (Supplementary Fig. 8b), memory testing. During the training phase of the RAWM all mice showed similar swim speeds (Supplementary Fig. 8c) and spatial learning capacity for the task (Fig 2e). However, during the testing phase animals administered with old plasma demonstrated impaired learning and memory for platform location (Fig 2e). As a control, we tested the RAWM paradigm in young adult mice with ablated hippocampal neurogenesis and observed corresponding behavioral deficits (Supplementary Fig. 9a–e). Collectively, these data indicate that factors present in aging blood inhibit adult neurogenesis, and moreover functionally contribute to impairments in cognitive function.

Thus far circulating factors associated with aging and tissue degeneration, or tissue rejuvenation, have remained elusive in earlier studies of parabiosis[19]. To identify such factors, we employed a proteomic approach in which relative levels of 66 cytokines, chemokines and other secreted signaling proteins were measured in the plasma of normal aging mice using standardized multiplex sandwich ELISAs (Luminex; Table S1). Using multivariate analysis, we identified seventeen proteins whose levels increased and correlated with decreased neurogenesis during aging (Fig 3a, Supplementary Fig. 10a,b). To identify systemic factors associated with heterochronic parabiosis, we analyzed plasma samples from young and old animals before and after pairings in an independent proteomic screen. Comparison of young isochronic and heterochronic cohorts identified fifteen factors that

increased in heterochronic parabionts (Fig. 3a, Supplementary Fig. 10c), while comparison between old isochronic and heterochronic cohorts revealed four factors that decreased in isochronic parabionts (Supplementary Fig. 10c). Interestingly, only six factors – CCL2, CCL11, CCL12, CCL19, Haptoglobin and β2-microglobulin – were elevated in old unpaired and young heterochronic cohorts (Fig 3a). CCL11, at the top of this list, is a chemokine involved in allergic responses and not previously linked to aging, neurogenesis, or cognition. Relative levels of CCL11 were increased in plasma of mice during normal aging (Fig 3b) and within young mice during heterochronic parabiosis (Fig. 3c). Furthermore, we detected an age-related increase in CCL11 in plasma (3d) and cerebrospinal fluid (CSF; Fig. 3e), from health human individuals between 20 and 90 years of age, suggesting that this age-related systemic increase is conserved across species.

Having identified CCL11 as an age-related systemic factor associated with decreased neurogenesis, we tested its potential biological relevance in vivo. We administered CCL11 protein through intraperitoneal injections into young adult Doublecortin-luciferase reporter mice[20], and using a non-invasive bioluminescent imaging assay detected a significant decrease in neurogenesis (Supplementary Fig. 11b,c). Using immunohistochemical analysis we investigated the effect of systemic CCL11 on adult hippocampal neurogenesis in young wild type adult mice. We administered CCL11 or vehicle alone, and in combination with either an anti-CCL11 neutralizing antibody or an isotype control antibody through intraperitoneal injections (Fig. 4a). Systemic administration of CCL11 induced an increase in CCL11 plasma levels (Supplementary Fig. 11a), and significantly decreased the number of Dcx-positive cells in the DG (Fig. 4b,c). Importantly, this decrease in neurogenesis could be rescued by systemic neutralization of CCL11 (Fig 4b,c). Likewise, BrdU-positive cells also showed similar changes in cell number (Supplementary Fig. 11d,e), and furthermore the percentage of cells expressing both BrdU and NeuN decreased (Supplementary Fig. 11f,g). The percentage of cells expressing BrdU and GFAP did not significantly change (Supplementary Fig. 11f,h). As a negative control we assayed neurogenesis after systemic administration of monocyte colony stimulating factor (MCSF), a measured protein not changing in plasma levels with age, and detected no change in Dcx-positive cells in the DG (Supplementary Fig. 12a–d). Together, these data indicate that increasing the systemic level of the age-related factor CCL11 is sufficient to partially recapitulate some of the inhibitory effects observed with aging and heterochronic parabiosis.

Additionally, we investigated the possibility that age-related blood-borne factors influence neural progenitor activity and neural differentiation in vitro. We assayed the number of neurospheres formed after exposure of primary NPCs to aged mouse serum and observed a 50% decrease when compared to young serum (Supplementary Fig. 13a). We then tested the effect of CCL11 and observed that the number and size of neurospheres formed from primary NPCs exposed to CCL11 significantly decreased (Supplementary Fig. 13b–d). Using a human derived NTERA cell line expressing eGFP under the Doublecortin promoter, we assayed neural differentiation and observed a significant decrease in eGFP expression after twelve days in culture with CCL11 (Supplementary Fig. 13e,f). While these findings open the possibility of a direct interaction of systemic factors with progenitor cells in vivo during aging, they do not preclude the possibility of indirect actions by interactions with other neurogenic niche cell types.

To examine the effect of CCL11 on neurogenesis in the brain we stereotaxically injected CCL11 into the DG of young adult mice, and observed a decrease in the number of Dcx-positive cells compared with the contralateral DG receiving vehicle control (Supplementary Fig. 14a,b). Furthermore, we examined whether the inhibitory effect of peripheral CCL11 could be restored locally within the hippocampus. We stereotaxically injected CCL11-specific neutralizing antibody and isotype control antibodies into the contralateral DG of young adult mice (Fig. 4d). Following stereotaxic injection, we systemically administered CCL11 or vehicle control by intraperitoneal injections (Fig. 4d). The decrease in Dcx-positive cell number observed in animals receiving systemic CCL11 administration could be rescued by neutralizing CCL11 within the DG (Fig. 4e,f), suggesting the increase in systemic chemokine levels exerts a direct effect in the CNS.

Finally, to determine the physiological relevance of increased systemic CCL11 levels in mice we assessed hippocampal dependent learning and memory using contextual fear conditioning and RAWM paradigms (Fig. 4g,h). Young adult mice received intraperitoneal injections of recombinant CCL11 or vehicle control. During fear conditioning training all mice, regardless of treatment, exhibited no differences in baseline freezing (Supplementary Fig. 15a). However, mice receiving CCL11 demonstrated decreased freezing during contextual (Fig. 4g), but not cued (Supplementary Fig. 15b), memory testing. During the training phase of the RAWM task all mice regardless of treatment showed similar swim speeds (Supplementary Fig. 15c) and learning capacity for the task (Fig. 4h). However, by the end of the testing phase animals receiving CCL11 exhibited impaired learning and memory deficits (Fig 4h). Together, these functional data demonstrate that increasing the systemic level of CCL11 cannot only inhibit adult neurogenesis, but also impair learning and memory.

Cumulatively, our data link age-related molecular changes in the systemic milieu to the age-related decline in adult neurogenesis, and impairments in synaptic plasticity and cognitive function observed during aging (Supplementary Fig. 1). While local immune signaling in the brain is emerging as a critical modulator of NPC function[11,15,21,22] and neurodegeneration[11,15,21], we now identify systemic immune-related factors as potentially critical contributors to the susceptibility of the aging brain to cognitive impairments. Interestingly, members of the identified age-related chemokines (CCL2, CCL11 and CCL12) are localized to within 70kB on mouse chromosome 11, and within 40kB on human chromosome 17, implicating this genetic locus in normal brain aging and possibly aging in general. Indeed, work investigating cellular senescence, a known hallmark of aging, furthers the involvement of some of the individual systemic chemokines reported here (CCL2) in the aging process as components of the Senescence-Associated Secretory Phenotype[23]. Lastly, while the proteomic platform we used here was sufficient to identify systemic inhibitory ‘aging’ factors it will be critical to develop and utilize broader proteomic screens to facilitate the discovery of systemic pro-neurogenic ‘rejuvenating’ factors with the potential to ameliorate age-related cognitive dysfunction.

Methods Summary

Animals: C57BL/6 (Jackson Laboratory), C57BL/6 aged mice (National Institutes of Aging), Dcx-Luc[20], and C57BL/6J-Act-GFP (Jackson Laboratory). All animal use was in accordance with institutional guidelines approved by the VA Palo Alto Committee on Animal Research. Parabiosis surgery followed previously described procedures[19] with the addition that peritonea between animals were surgically connected. Immunohistochemistry followed standard published techniques[24]. Extracellular electrophysiology was performed as previously described[25]. Spatial learning and memory was assayed with the RAWM paradigm as previously published[26]. Contextual fear conditioning was assayed as previously published[27]. Relative plasma concentrations of cytokines and signaling molecules in mice and humans were measured using antibody-based multiplex immunoassays at Rules Based Medicine, Inc. Statistical analysis was performed with Prism 5.0 software (GraphPad Software). Plasma protein correlations were analyzed with the Significance Analysis of Microarray software (*SAM 3.00* algorithm; http://www.stat.stanford.edu/~tibs/SAM/index.htm). Experiments were carried out by investigators blinded to the treatment of animals.

Methods

Mice

The following mouse lines were used: C57BL/6 (The Jackson Laboratory), C57BL/6 aged mice (National Institutes of Aging), Dcx-Luc mice[20], and C57BL/6J-Act-GFP (Jackson Laboratory). For parabiosis experiments male and female C57BL/6 mouse cohorts were used. For all other in vivo pharmacological and behavioral studies young (2–3 months) wild type C57BL/6 male mice were used. Mice were housed under specific pathogen-free conditions under a 12 h light-dark cycle and all animal handling and use was in accordance with institutional guidelines approved by the VA Palo Alto Committee on Animal Research.

Immunohistochemistry

Tissue processing and immunohistochemistry was performed on free-floating sections following standard published techniques[24]. Briefly, mice were anesthetized with 400 mg/kg chloral hydrate (Sigma-Aldrich) and transcardially perfused with 0.9% saline. Brains were removed and fixed in phosphate-buffered 4% paraformaldehyde, pH 7.4, at 4°C for 48 h before they were sunk through 30% sucrose for cryoprotection. Brains were then sectioned coronally at 40 μm with a cryomicrotome (Leica Camera, Inc.) and stored in cryoprotective medium. Primary antibodies were: goat anti-Dcx (1:500; Santa Cruz Biotechnology), rat anti-BrdU (1:5000, Accurate Chemical and Scientific Corp.), goat anti-Sox2 (1:200; Santa Cruz), mouse anti-NeuN (1:1000, Chemicon), mouse anti-GFAP (1:1500, DAKO), and mouse anti-CD68 (1:50, Serotec). After overnight incubation, primary antibody staining was revealed using biotinylated secondary antibodies and the ABC kit (Vector) with Diaminobenzidine (DAB, Sigma-Aldrich) or fluorescence conjugated secondary antibodies. For BrdU labeling, brain sections were pre-treated with 2N HCl at 37°C for 30 min before incubation with primary antibody. For double-label immunofluorescence of BrdU/NeuN or BrdU/GFAP, sections were incubated overnight with rat anti-BrdU, rinsed, and incubated

for 1hr with donkey anti-rat antibody (2.5 μg/ml, Vector) before they were stained with mouse anti-NeuN antibody. To estimate the total number of Dcx or Sox2 positive cells per DG immunopositive cells in the granule cell and subgranular cell layer of the DG were counted in every sixth coronal hemibrain section through the hippocampus and multiplied by 12.

BrdU administration and quantification of BrdU-positive cells

50 mg/kg of BrdU was injected intraperitoneally into mice once a day for 6 days, and mice were sacrificed 28 days later or injected daily for 3 days before sacrifice. To estimate the total number of BrdU-positive cells in the brain, we performed DAB staining for BrdU on every sixth hemibrain section. The number of BrdU+ cells in the granule cell and subgranular cell layer of the DG were counted and multiplied by 12 to estimate the total number of BrdU-positive cells in the entire DG. To determine the fate of dividing cells a total of 200 BrdU-positive cells across 4–6 sections per mouse were analyzed by confocal microscopy for co-expression with NeuN and GFAP. The number of double-positive cells was expressed as a percentage of BrdU- positive cells.

Parabiosis and flow cytometry

Parabiosis surgery followed previously described procedures[19]. Pairs of mice were anesthetized and prepared for surgery. Mirror-image incisions at the left and right flanks, respectively, were made through the skin. Shorter incisions were made through the abdominal wall. The peritoneal openings of the adjacent parabionts were sutured together. Elbow and knee joints from each parabiont were sutured together and the skin of each mouse was stapled (9mm Autoclip, Clay Adams) to the skin of the adjacent parabiont. Each mouse was injected subcutaneously with Baytril antibiotic and Buprenex as directed for pain and monitored during recovery. Flow cytometric analysis was done on fixed and permeabilized blood plasma cells from GFP and non-GFP parabionts. Approximately 40–60% of cells in the blood of either parabiont were GFP-positive two weeks after parabiosis surgery. We observed 70–80% survival rate in parabionts five weeks post parabiosis surgery.

Extracellular Electrophysiology

Acute hippocampal slices (400 μm thick) were prepared from unpaired and young parabionts. Slices were maintained in artificial cerebrospinal fluid (ACSF) continuously oxygenated with 5% CO_2/95% O_2. ACSF composition was as follows: (in mM): NaCl 124.0; KCl 2.5; KH_2PO4 1.2; $CaCl_2$ 2.4; $MgSO_4$ 1.3; $NaHCO_3$ 26.0; glucose 10.0 (pH 7.4). Recordings were performed with an Axopatch- 2B amplifier and pClamp 10.2 software (Axon Instruments). Submerged slices were continuously perfused with oxygenated ACSF at a flow rate of 2 ml/min from a reservoir by gravity feeding. Field potential (population spikes and EPSP) was recorded using glass microelectrodes filled with ACSF (resistance: 4–8 MΩ). Biphasic current pulses (0.2 ms duration for one phase, 0.4ms in total) were delivered in 10 s intervals through a concentric bipolar stimulating electrode (FHC, Inc.). No obvious synaptic depression or facilitation was observed with this frequency stimulation. To record field population spikes in the dentate gyrus, the recording electrode was placed in the lateral or medial side of the dorsal part of the dentate gyrus. The stimulating electrode was

placed right above the hippocampal fissure to stimulate the perforant pathway fibers. Signals were filtered at 1 KHz and digitized at 10 KHz. Tetanic stimulation consisted of 2 trains of 100 pulses (0.4 ms pulse duration, 100 Hz) delivered with an inter-train interval of 5 seconds. The amplitude of population spike was measured from the initial phase of the negative wave. Up to five consecutive traces were averaged for each measurement. Synaptic transmission was assessed by generating input-output curves, with stimulus strength adjusted to be ~30% of the maximum. LTP was calculated as mean percentage change in the amplitude of the population spike following high frequency stimulation relative to its basal amplitude.

Contextual Fear Conditioning

Paradigm was done following previously published techniques[27]. In this task, mice learned to associate the environmental context (fear conditioning chamber) with an aversive stimulus (mild foot shock; unconditioned stimulus, US) enabling testing for hippocampal-dependent contextual fear conditioning. As contextual fear conditioning is hippocampus and amygdala dependent, the mild foot shock was paired with a light and tone cue (conditioned stimulus, CS) in order to also assess amygdala-dependent cued fear conditioning. Conditioned fear was displayed as freezing behavior. Specific training parameters are as follows: tone duration is 30 seconds; level is 70 dB, 2 kHz; shock duration is 2 seconds; intensity is 0.6 mA. This intensity is not painful and can easily be tolerated but will generate an unpleasant feeling. More specifically, on day 1 each mouse was placed in a fear-conditioning chamber and allowed to explore for 2 minutes before delivery of a 30-second tone (70 dB) ending with a 2-second foot shock (0.6mA). Two minutes later, a second CS-US pair was delivered. On day 2 each mouse was first place in the fear-conditioning chamber containing the same exact context, but with no adminstration of a CS or foot shock. Freezing was analyzed for 1–3 minutes. One hour later, the mice were placed in a new context containing a different odor, cleaning solution, floor texture, chamber walls and shape. Animals were allowed to explore for 2 minutes before being re-exposed to the CS. Freezing was analyzed for 1–3 minutes. Freezing was measured using a FreezeScan video tracking system and software (Cleversys, Inc).

Radial Arm Water Maze

Spatial learning and memory was assessed using the radial arm water maze (RAWM) paradigm following the exact protocol described by Alamed et al.[26]. The goal arm location containing a platform remains constant throughout the training and testing phase, while the start arm is changed during each trial. On day one during the training phase, mice are trained for 15 trials, with trials alternating between a visible and hidden platform. On day two during the testing phase, mice are tested for 15 trials with a hidden platform. Entry into an incorrect arm is scored as an error, and errors are averaged over training blocks (three consecutive trials).

Cranial Irradiation

Adult mice (8–12 weeks) were sham irradiated (controls) or irradiated at 5 Gy three times over eight days using the Mark I gamma irradiator and sacrificed at 8–10 weeks after irradiation to collect brains for immunohistochemical analyses. Each mouse was placed in a

restrainer that was fitted into a slot in the lead brick shield so that the back of the skull was facing the source of radiation when positioned in the radiation chamber. The shield is constructed of lead bricks such that only the hippocampal/midbrain area were exposed to radiation. Calibration for 5 Gy radiation was done using nanoDot. Shielded areas were protected with an exposure rate 10 times lower than the exposed area. RAWM studies were done on irradiated mice at least 6 weeks after the radiation procedure. This time frame ensured adequate recovery of the animals. All data were from 8 irradiated and 10 sham irradiated mice.

Plasma collection and proteomic analysis

Mouse blood was collected from 400–500 young (2–3 months) and old (18–22 months) animals into EDTA coated tubes via tail vein bleed, mandibular vein bleed, or intracardial bleed at time of sacrifice. EDTA plasma was generated by centrifugation of freshly collected blood and aliquots were stored at −80°C until use. Human plasma and CSF samples were obtained from academic centers and subjects were chosen based on standardized inclusion and exclusion criteria as previously described[28,29]. The relative plasma concentrations of cytokines and signaling molecules were measured in human and mouse plasma samples using standard antibody-based multiplex immunoassays (Luminex) by either Rules Based Medicine Inc., a fee-for-service provider, or by the Human Immune Monitoring Center at Stanford University. All Luminex measurements where obtained in a blinded fashion. All assays were developed and validated to Clinical Laboratory Standards Institute (formerly NCCLS) guidelines based upon the principles of immunoassay as described by the manufacturers.

CCL11, MSCF, antibody, or plasma administration

Carrier free recombinant murine CCL11 dissolved in PBS (10ug/kg; R&D Systems), carrier free recombinant MCSF dissolved in PBS (10ug/kg; Biogen), rat IgG2a neutralizing antibody against mouse CCL11 (50ug/ml; R&D Systems, Clone: 42285), and isotype matched control rat IgG2a recommended by the manufacturer (R&D Systems, Clone: 54447) were administered systemically via intraperitoneal injection over ten days on day 1, 4, 7, and 10. The same reagents (0.50ul; 0.1ug/ul) were also administered stereotaxically into the DG of the hippocampus in some experiments (coordinates from bregma: A = −2.0mm and L = −1.8mm, from brain surface: H = −2.0mm). Pooled mouse serum or plasma was collected from young (2–3 months) mice and old (18–20 months) mice by intracardial bleed at time of sacrifice. Serum was prepared from clotted blood collected without anticoagulants; plasma was prepared from blood collected with EDTA followed by centrifugation. Aliquots were stored at −80°C until use. Prior to administration plasma was dialyzed in PBS to remove EDTA. Young adult mice were systemically treated with plasma (100ul) isolated from young or aged mice via intravenous injections four times over ten days.

In vivo bioluminescence imaging

Bioluminescence was detected with the In Vivo Imaging System (IVIS Spectrum; Caliper Life Science). Mice were injected intraperitoneally with 150mg/kg D-luciferin (Xenogen) 10 minutes before imaging and anesthetized with isofluorane during imaging. Photons emitted

from living mice were acquired as photons/s/cm^2/steridan (sr) using LIVINGIMAGE software (version 3.5, Caliper) and integrated over 5 minutes. For quantification a region of interest was manually selected and kept constant for all experiments.

Cell culture assays

Mouse neural progenitor cells were isolated from C57BL/6 mice as previously described[12]. Brains from postnatal animals (1 day-old) were dissected to remove olfactory bulb, cerebellum and brainstem. After removing superficial blood vessels forebrains were finely minced, digested for 30 minutes at 37°C in DMEM media containing 2.5U/ml Papain (Worthington Biochemicals), 1U/ml Dispase II (Boeringher Mannheim), and 250U/ml DNase I (Worthington Biochemicals) and mechanically dissociated. NSC/progenitors were purified using a 65% Percoll gradient and plated on uncoated tissue culture dishes at a density of 10^5 cells/cm^2. NPCs were cultured under standard conditions in NeuroBasal A medium supplemented with penicillin (100U/ml), streptomycin (100mg/ml), 2 mM L-glutamine, serum-free B27 supplement without vitamin A (Sigma-Aldrich), bFGF (20ng/ml) and EGF (20ng/ml). Carrier free forms of murine recombinant CCL2 (100ng/ml; R&D Systems), murine recombinant CCL11 (100 ng/ml, R&D Systems), rat IgG2b neutralizing antibody against mouse CCL2 (10ug/ml; R&D Systems, Clone: 123616), control rat IgG2b (10ug/ml; R&D Systems, Clone: 141945), goat IgG neutralizing antibody against mouse CCL11 (10ug/ml; R&D Systems), and control goat IgG (10ug/ml; R&D Systems) were dissolved in PBS and added to cell cultures under self-renewal conditions every other day following cell plating.

Human NTERA cells[7] expressing eGFP under the doublecortin promoter were cultured under standard self-renewal and differentiation conditions[30,31]. Carrier free forms of human recombinant CCL2 (100ng/ml, R&D Systems), human recombinant CCL11 (100 ng/ml, R&D Systems), mouse IgG_1 neutralizing antibody against human CCL11 (25ug/ml; R&D Systems, Clone: 43911) and control mouse IgG_1 (25ug/ml; R&D Systems) were added to cell cultures under differentiation conditions every other day following cell plating.

Data and statistical analysis

Data are expressed as mean ± SEM. Statistical analysis was performed with Prism 5.0 software (GraphPad Software). Means between two groups were compared with two-tailed, unpaired Student's t test. Comparisons of means from multiple groups with each other or against one control group were analyzed with 1-way ANOVA and Tukey-Kramer's or Dunnett's post hoc tests, respectively. Plasma protein correlations in the aging samples were analyzed with the Significance Analysis of Microarray software (*SAM 3.00* algorithm; http://www.stat.stanford.edu/~tibs/SAM/index.htm). Unsupervised cluster analysis was performed using Gene Cluster 3.0 software and node maps were produced using Java TreeView 1.0.13 software. All histology, electrophysiology and behavior experiments conducted were done in a randomized and blinded fashion.

Supplementary Material

Refer to Web version on PubMed Central for supplementary material.

Acknowledgments

We thank Dr. Anne Brunet for critically reading the manuscript; Dr. Marion Buckwalter for parabiosis instruction; Dr. Ting-Ting Huang for irradiation instruction; Dr. Rikki Corniola and Dr. Claire Clelland for behavioral advice, Dr. Sarah Bauer Huang, Hudson Johns, Johnny Sun, Hugh Hefner, Haitham Alabsi and Idalia Villeda for technical assistance. We are grateful to numerous unnamed human subjects and staff for their contributions. This work was supported by grants from Anonymous (T.W.-C), Department of Veterans Affairs (T.W.-C), National Institutes of Health Institute on Aging (R01 AG027505, T.W.-C), a California Initiative for Regenerative Medicine Award (T.W.-C), National Institutes of Health (R01 MH078194, X.S.X), National Institutes of Health Institute on Aging (P30 AG08017, J.A.K), a National Institutes of Health Director's Pioneer Award (T.A.R), a Larry L. Hillblom Foundation postdoctoral fellowship (K.M.L; 2008-A-023-FEL), a Feodor-Lynen postdoctoral fellowship (E.C), a Swiss National Science Foundation postdoctoral fellowship (A.E.), a National Science Foundation predoctoral fellowship (S.A.V; K.I.M; T.M.S), a Kirschstein NRSA predoctoral fellowships (1 F31 AG034045-01, S.A.V; 1 F31 NS066676-01A1, Z.D).

References

1. van Praag H, Shubert T, Zhao C, Gage FH. Exercise enhances learning and hippocampal neurogenesis in aged mice. J Neurosci. 2005; 25 (38):8680–8685. [PubMed: 16177036]
2. Gage FH. Mammalian neural stem cells. Science. 2000; 287 (5457):1433–1438. [PubMed: 10688783]
3. Alvarez-Buylla A, Lim DA. For the long run: maintaining germinal niches in the adult brain. Neuron. 2004; 41 (5):683–686. [PubMed: 15003168]
4. Zhao C, Deng W, Gage FH. Mechanisms and functional implications of adult neurogenesis. Cell. 2008; 132 (4):645–660. [PubMed: 18295581]
5. van Praag H, et al. Functional neurogenesis in the adult hippocampus. Nature. 2002; 415 (6875): 1030–1034. [PubMed: 11875571]
6. Deng W, Aimone JB, Gage FH. New neurons and new memories: how does adult hippocampal neurogenesis affect learning and memory? Nat Rev Neurosci. 11(5):339–350. [PubMed: 20354534]
7. Clelland CD, et al. A functional role for adult hippocampal neurogenesis in spatial pattern separation. Science. 2009; 325 (5937):210–213. [PubMed: 19590004]
8. Zhang CL, Zou Y, He W, Gage FH, Evans RM. A role for adult TLX-positive neural stem cells in learning and behaviour. Nature. 2008; 451 (7181):1004–1007. [PubMed: 18235445]
9. Saxe MD, et al. Ablation of hippocampal neurogenesis impairs contextual fear conditioning and synaptic plasticity in the dentate gyrus. Proc Natl Acad Sci U S A. 2006; 103 (46):17501–17506. [PubMed: 17088541]
10. Shen Q, et al. Endothelial cells stimulate self-renewal and expand neurogenesis of neural stem cells. Science. 2004; 304 (5675):1338–1340. [PubMed: 15060285]
11. Carpentier PA, Palmer TD. Immune influence on adult neural stem cell regulation and function. Neuron. 2009; 64 (1):79–92. [PubMed: 19840551]
12. Renault VM, et al. FoxO3 regulates neural stem cell homeostasis. Cell Stem Cell. 2009; 5 (5):527–539. [PubMed: 19896443]
13. Molofsky AV, et al. Increasing p16INK4a expression decreases forebrain progenitors and neurogenesis during ageing. Nature. 2006; 443 (7110):448–452. [PubMed: 16957738]
14. Lie DC, et al. Wnt signalling regulates adult hippocampal neurogenesis. Nature. 2005; 437 (7063): 1370–1375. [PubMed: 16251967]
15. Lucin KM, Wyss-Coray T. Immune activation in brain aging and neurodegeneration: too much or too little? Neuron. 2009; 64 (1):110–122. [PubMed: 19840553]
16. Rapp PR, Heindel WC. Memory systems in normal and pathological aging. Curr Opin Neurol. 1994; 7 (4):294–298. [PubMed: 7952236]
17. Ajami B, Bennett JL, Krieger C, Tetzlaff W, Rossi FM. Local self-renewal can sustain CNS microglia maintenance and function throughout adult life. Nat Neurosci. 2007; 10 (12):1538–1543. [PubMed: 18026097]
18. Bliss TV, Collingridge GL. A synaptic model of memory: long-term potentiation in the hippocampus. Nature. 1993; 361 (6407):31–39. [PubMed: 8421494]

19. Conboy IM, et al. Rejuvenation of aged progenitor cells by exposure to a young systemic environment. Nature. 2005; 433 (7027):760–764. [PubMed: 15716955]
20. Couillard-Despres S, et al. In vivo optical imaging of neurogenesis: watching new neurons in the intact brain. Mol Imaging. 2008; 7 (1):28–34. [PubMed: 18384721]
21. Monje ML, Toda H, Palmer TD. Inflammatory blockade restores adult hippocampal neurogenesis. Science. 2003; 302 (5651):1760–1765. [PubMed: 14615545]
22. Moriyama M, et al. Complement receptor 2 is expressed in neural progenitor cells and regulates adult hippocampal neurogenesis. J Neurosci. 31(11):3981–3989. [PubMed: 21411641]
23. Fumagalli M, d'Adda di Fagagna F. SASPense and DDRama in cancer and ageing. Nat Cell Biol. 2009; 11 (8):921–923. [PubMed: 19648977]
24. Luo J, et al. Glia-dependent TGF-beta signaling, acting independently of the TH17 pathway, is critical for initiation of murine autoimmune encephalomyelitis. J Clin Invest. 2007; 117 (11): 3306–3315. [PubMed: 17965773]
25. Xie X, Smart TG. Modulation of long-term potentiation in rat hippocampal pyramidal neurons by zinc. Pflugers Arch. 1994; 427 (5–6):481–486. [PubMed: 7971146]
26. Alamed J, Wilcock DM, Diamond DM, Gordon MN, Morgan D. Two-day radial-arm water maze learning and memory task; robust resolution of amyloid-related memory deficits in transgenic mice. Nat Protoc. 2006; 1 (4):1671–1679. [PubMed: 17487150]
27. Raber J, et al. Irradiation enhances hippocampus-dependent cognition in mice deficient in extracellular superoxide dismutase. Hippocampus. 21(1):72–80. [PubMed: 20020436]
28. Zhang J, et al. CSF multianalyte profile distinguishes Alzheimer and Parkinson diseases. Am J Clin Pathol. 2008; 129 (4):526–529. [PubMed: 18343778]
29. Li G, et al. Cerebrospinal fluid concentration of brain-derived neurotrophic factor and cognitive function in non-demented subjects. PLoS One. 2009; 4 (5):e5424. [PubMed: 19412541]
30. Couillard-Despres S, et al. Human in vitro reporter model of neuronal development and early differentiation processes. BMC Neurosci. 2008; 9:31. [PubMed: 18312642]
31. Buckwalter MS, et al. Chronically increased transforming growth factor-beta1 strongly inhibits hippocampal neurogenesis in aged mice. Am J Pathol. 2006; 169 (1):154–164. [PubMed: 16816369]

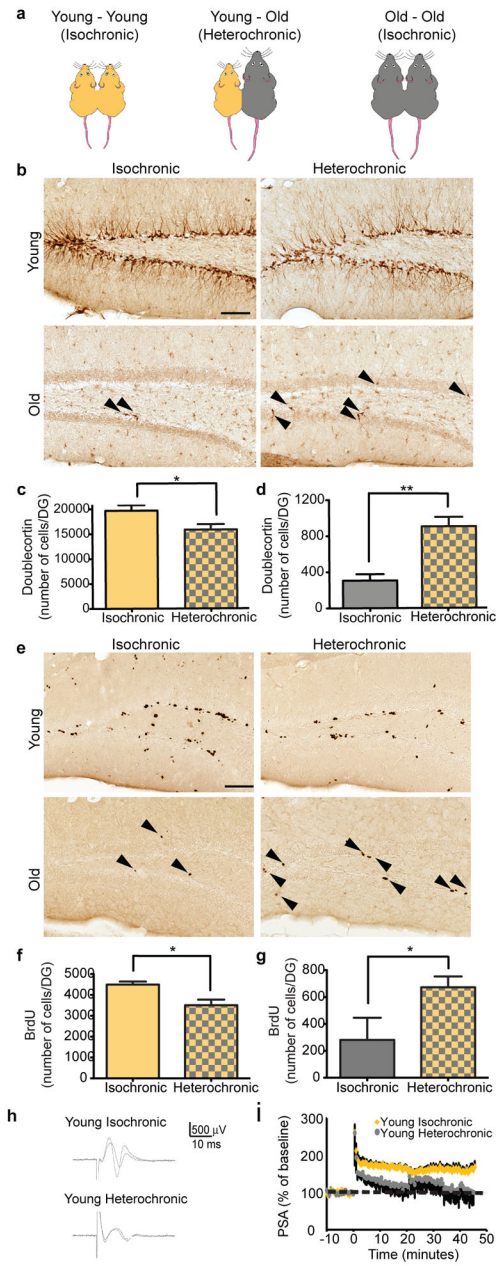

Figure 1. Heterochronic parabiosis alters neurogenesis in an age-dependent fashion

a, Schematic showing parabiotic pairings. **b,e,** Representative fields of Doublecortin (**b**) and BrdU (**e**) immunostaining of young (3–4 months; yellow) and old (18–20 months; gray) isochronic and heterochronic parabionts five weeks after parabiosis (arrowheads point to individual cells, scale bar: 100μm). **c–f** Quantification of neurogenesis (**c,d**) and proliferating cells (**e,f**) in the young (**c,e**; top) and old (**d,f**; bottom) DG after parabiosis. Data from 12 young isochronic, 10 young heterochronic, 6 old isochronic and 12 old heterochronic parabionts. **g,h,** Population spike amplitude (PSA) was recorded from DG of young parabionts. Representative electrophysiological profiles (**g**) and LTP levels (**h**) are

shown for young heterochronic and isochronic parabionts. Data from 4–5 mice per group. All data represented as Mean + SEM; *P<0.05; **P<0.01 t-test.

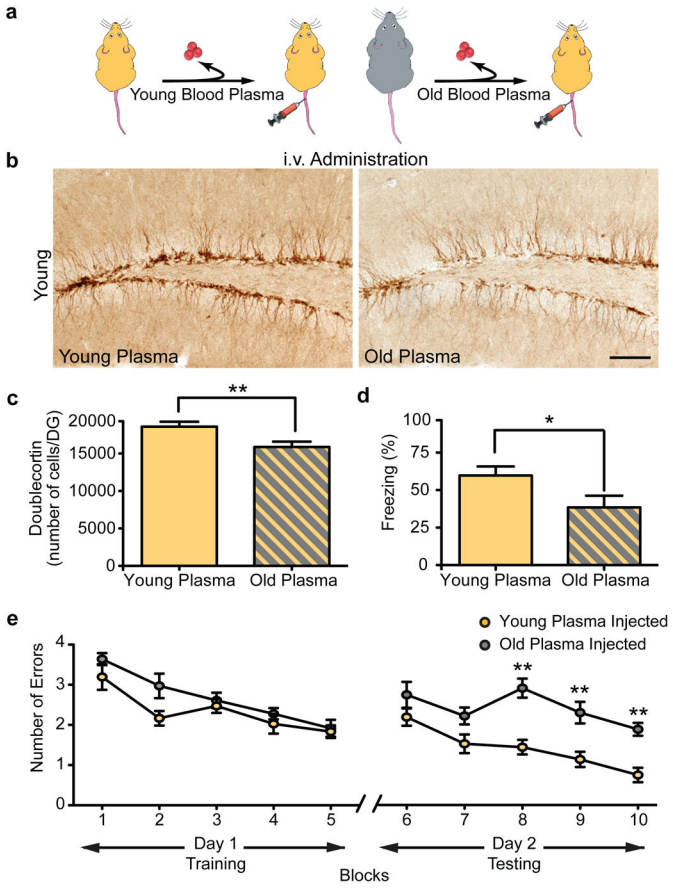

Figure 2. Factors from an old systemic environment decrease neurogenesis and impair learning and memory

a, Schematic of young (3–4 months) or old (18–22 months) plasma extraction and intravenous injection into young (3 months) adult mice. **b,** Representative field of Doublecortin immunostaining of young adult mice after plasma injection treatment four times over ten days (scale bar: 100μm). **c,** Quantification of neurogenesis in the young DG after plasma injection. Data from 8 young plasma and 7 old plasma injected mice. **d,e** Hippocampal learning and memory assessed by contextual fear conditioning (**d**) and RAWM (**e**) paradigms in young adult mice after young or old plasma injections nine times over 24 days. **d**, Percent freezing time 24 hours after training. Data from 8 mice per group. **e**, Number of entry arm errors prior to finding platform. Data from 12 mice per group. All data represented as Mean ± SEM; **P*< 0.05; ***P*< 0.01; t-test (**c,d**), repeated measures ANOVA, Bonferroni post-hoc test (**e**).

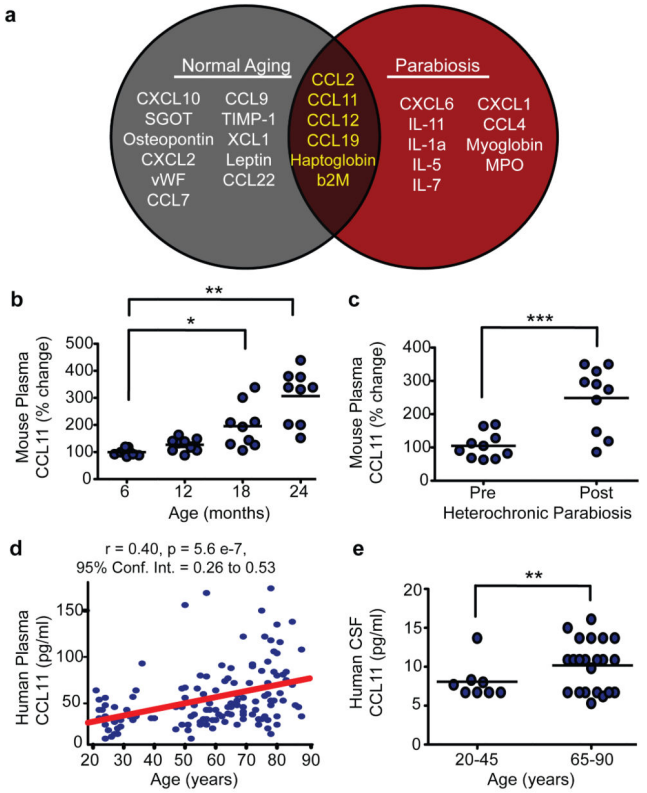

Figure 3. Systemic chemokine levels increase during aging and heterochronic parabiosis and correlate with decreased neurogenesis

a, Venn diagram of results from aging and parabiosis proteomic screens. Seventeen age-related plasma factors correlated strongest with decreased neurogenesis in gray, fifteen plasma factors increased between young isochronic and young heterochronic parabionts in red, and six factors elevated in both screens in brown intersection. Data from 5–6 animals per age group. **b,c** Changes in plasma concentrations of CCL11 with age (**b**) and young heterochronic parabionts pre- and post- parabiotic pairing (**c**). **d,e** Changes in plasma (**d**) and CSF (**e**) concentrations of CCL11 with age in healthy human subjects. All data represented as dot plots with mean; **P*< 0.05; ***P*< 0.01; ****P*< 0.001 t-test (**c,e**), ANOVA, Tukey's post-hoc test (**a,b**), and Mann-Whitney U Test (**d**).

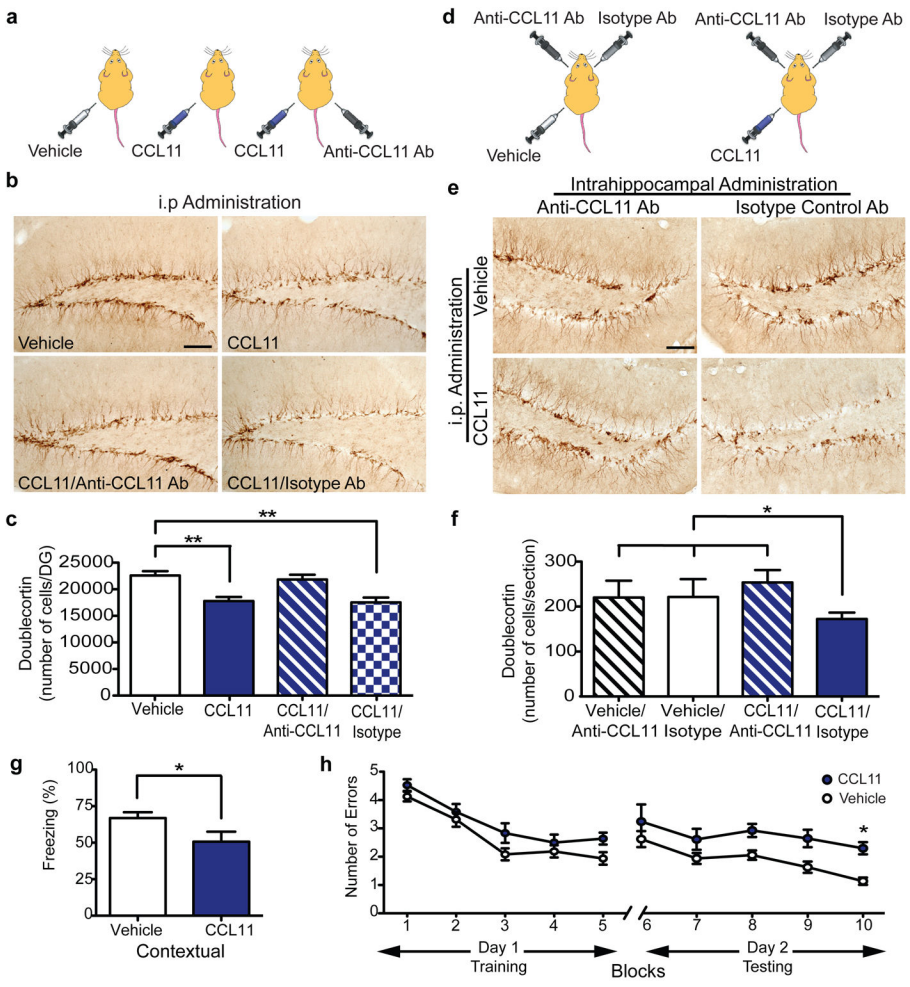

Figure 4. Systemic exposure to CCL11 inhibits neurogenesis and impairs learning and memory

a, Schematic of young (3–4 months) mice injected intraperitoneally with CCL11 or vehicle, and in combination with anti-CCL11 neutralizing or isotype control antibody. **b,** Representative field of Dcx-positive cells for each treatment group (n = 6–10 mice) treated four times over ten days. (scale bar: 100μm). **c,** Quantification of neurogenesis in the DG after treatment. **d,** Schematic of young adult mice given unilateral stereotaxic injections of anti-CCL11 neutralizing or isotype control antibody followed by systemic injections with either recombinant CCL11 or PBS (vehicle). **e,** Representative field of Dcx-positive cells in adjacent sides of the DG for each treatment group (n = 3–11 mice) **f,** Quantification of neurogenesis in the DG after systemic and stereotaxic treatment. **g,h,** Learning and memory assessed by contextual fear conditioning (**g**) and RAWM (**h**) paradigms in young adult mice injected with CCL11 or vehicle every three days for five weeks (n = 12–16 mice per group). All data represented as Mean ± SEM; **P*< 0.05; ***P*<0.01; ANOVA, Dunnet's or Tukey's post-hoc test (**c,f**); repeated measures ANOVA, Bonferroni post-hoc test (**k**).